VERTEBRATE ZOOLOGY

69 (3): 311–325
2019

SENCKENBERG

Cranial osteology and molecular phylogeny of *Argyrogena fasciolata* (Shaw, 1802) (Colubridae: Serpentes)

Sunandan Das[1,6], Patrick D. Campbell[2], Souparno Roy[1,3], Souryadeep Mukherjee[1], Kousik Pramanick[1], Amit Biswas[4], Sujoy Raha[5]

[1] Department of Life Sciences, Presidency University, Kolkata – 700073, West Bengal, India — [2] Department of Life Sciences, Darwin Centre, Natural History Museum, Cromwell Road, South Kensington, London SW7 5BD, England — [3] Nature Mates – Nature Club, 6/7 Bijoygarh, Jadavpur, Kolkata-700032, West Bengal, India — [4] Paschim Digher Par, Canning-743329, West Bengal, India — [5] Reptilia Section, Zoological Survey of India, Fire-proof Spirit Building, Kolkata-700016, West Bengal, India — [6] Corresponding author: sdassnake@gmail.com

Submitted January 3, 2019.
Accepted July 30, 2019.
Published online at www.senckenberg.de/vertebrate-zoology on August 15, 2019.
Published in print Q4/2019.

Editor in charge: Uwe Fritz

Abstract

Descriptive accounts of the cranial osteology of snakes is important for systematics, functional morphology and also, to some extent, palaeontology. In the present study, we describe the skull of *Argyrogena fasciolata*, a south Asian colubrid snake, in detail. Bones of the snout unit of this snake are adapted for a fossorial mode of life whereas the braincase lacks any adaptations related to such an existence. We also compared its skull with other snakes belonging to sixteen other genera which together form the large clade containing Afrotropical, Palaearctic and Saharo-Arabian racers/whip snakes. The comparison shows that the cranium of *A. fasciolata* bears more similarity with that of *Platyceps* spp, differing mostly in three characteristics pertaining to premaxilla, nasal and pterygoid bones, than it does with crania of other genera. This suggests a closer relationship between those two genera. We also performed molecular phylogenetic analyses on three mitochondrial loci using Maximum Likelihood and Bayesian Inference optimality criteria. The resultant phylogenies indeed recover *A. fasciolata* as sister to *Platyceps* spp.

Key words

Argyrogena, Skull, Molecular phylogeny, Colubridae, Systematics, *Platyceps*.

Introduction

Argyrogena fasciolata (Shaw, 1802), commonly known as the banded racer, is a colubrid snake endemic to the Indian subcontinent, being found in India, southeastern Pakistan, Nepal, northern Sri Lanka and Bangladesh (Smith, 1943; Minton, 1966; Mertens, 1969; Whitaker & Captain, 2004; Das & Silva, 2005; Wallach *et al*., 2014). Since its first description as *Coluber fasciolatus*, it has been assigned variously to different genera. Günther (1858) initially assigned it to *Coryphodon* but he subsequently (1864) transferred it to *Zamenis*, recognizing its 'Mediterranean' affinities. Boulenger (1890, 1893) also used *Zamenis* for this species but his *Zamenis* was, to some extent, a catch-all genus for several rather distantly related snakes. Authors in the first half of the last century have classified it under either *Zamenis* (e.g. Wall, 1913, 1921) or *Coluber* (e.g. Smith, 1943; Constable, 1949). Smith (1943) included those species in *Coluber* which are currently classified under genera *Hemorrhois*, *Platyceps* and *Spalerosophis* and thus his scheme reflects the phylogenetic relationships better (these genera are indeed found to form a monophyletic clade in recent studies [e.g. Schätti & Utiger, 2001; Utiger *et al*., 2005]). Wilson (1967) studied *Coluber fasciolatus* and felt the need to classify it under a monotypic genus. Werner's (1924) *Argyrogena* (type *A. rostrata*, a junior subjective synonym of *C. fasciolatus* according to Smith [1928]) was available to serve that purpose. Since then most workers (e.g. Whitaker

& Captain, 2004; Wallach *et al*., 2014) followed Wilson in calling this species *Argyrogena fasciolata*. Utiger *et al*. (2005) suggested that *A. fasciolata* belongs to the clade of racers / whip snakes of predominantly Afrotropical, Saharo-Sindian and Palaearctic distribution (zoogeographic classification follows Holt *et al*. [2012]). However, though the close relationship of this snake with the racer / whip snake genera from the aforesaid realms has been recognized either implicitly or explicitly by many authors, its exact phylogenetic relationships remain unknown. Even though two mitochondrial loci from this species were sequenced in a barcoding study (Khedkar *et al*., 2014), the sequences were not analyzed in the context of other racers / whip snakes. Therefore, an investigation into the evolutionary relationships of *A. fasciolata* is required.

Information on cranial osteology is of importance in studies focusing on systematics, functional morphology, study of trait evolution and also, to a certain extent, palaeoherpetology. Identification of recent fossil materials of squamates depends on skeletal anatomical data of extant taxa (Bell & Mead, 2014). Fraser (1937) gave a very short, incomplete and somewhat inaccurate description of the cranium of *A. fasciolata*. Smith (1943) illustrated a maxilla whereas Wilson (1967) illustrated a pterygoid and provided a cursory description of a few bones for the sake of comparison. Hence, it can be seen that accurate information available from literature on the cranial osteology of this snake is rather sparse. Moreover, absolutely no information on the variation of skull bones (except number of teeth) is available even though data on intraspecific variation in cranial osteological features is of much importance (Szyndlar & Rage, 2002; Bell & Mead, 2014). Hence, a detailed account of the cranial osteology of *A. fasciolata*, including the description of intraspecific variation, is also highly warranted.

In the present study, we provide a detailed description of the cranial osteology of *A. fasciolata*. A comparison with the cranial features of other racers has also been given. We also investigate the phylogenetic relationships of this species using data from three mitochondrial loci and provide a discussion on its generic taxonomy.

Material and Methods

We studied dry osteological material either directly or from high quality photographs. All studied materials (see Appendix 1 for a list) belong to the holdings of following museums (abbreviations in parenthesis) – Natural History Museum, London (NHMUK), American Museum of Natural History, New York City (AMNH), Field Museum of Natural History, Chicago (FMNH), Louisiana State University Museum of Natural Science, Baton Rouge (LSUMNS), Presidency University Zoology Museum, Kolkata (PUZ) and University of Michigan Zoology Museum, Ann Arbor (UMMZ; materials belonging to this collection were studied from microCT scans on MorphoSource). Studied materials (including MorphoSource media numbers and voucher specimen for molecular work) are listed in Appendix 1. No specimens have been collected or killed for the present study. Characters were noted with a Zeiss Stemi 2000C dissecting binocular microscope. Terminology used in the present work for cranial osteological features follow mostly Cundall & Irish (2008), Underwood (1967) and McDowell (2008). Citations were made at appropriate places whenever we used terminology derived from works other than the aforementioned ones.

Whole genomic DNA was extracted from liver tissue dissected out from an ethanol preserved museum specimen (see Appendix 1) of *Argyrogena fasciolata* following the Phenol-Chloroform extraction protocol. PCR primers for amplification of mitochondrial 12s ribosomal DNA and PCR conditions follow Schätti & Utiger (2001) and Sinaiko *et al*. (2018). PCR products were visualized in 1% agarose gel, purified with a Thermo Scientific GeneJet PCR purification kit following the protocol provided by the manufacturer and then Sanger sequenced. The sequence has been deposited in GenBank under accession number MK329299.

Sequences of mitochondrial 16S ribosomal RNA and cytochrome C oxidase, subunit I (COI) genes of *Argyrogena fasciolata* were obtained from the Barcode of Life Database (BOLD systems) (Ratnasingham & Hebert, 2007). Sequences of the three aforesaid genes for all genera which were recovered within the clade of Afro-Tropical, Palaearctic and Saharo-Arabian racer / whip snakes in recent, large scale studies (Pyron *et al*., 2013; Figueroa *et al*., 2016), were downloaded from GenBank. Three Oriental rat / trinket snakes of genera *Coelognathus*, *Elaphe* and *Ptyas* were also added. *Natrix natrix* was used as the outgroup to root the phylogenetic tree. The BOLD and GenBank numbers of the sequences are provided in Appendix 2. The sequences were aligned with clustalW (Thompson *et al*., 1994) in MEGA X (Kumar *et al*., 2018). The alignments were checked with eye and adjustments were made where necessary. The alignments were trimmed where necessary and then concatenated in sequencematrix 1.8 (Vaidya *et al*., 2011). The concatenated dataset was 1973 bp long. Partitioning scheme for this dataset (Table 1) was determined on the basis of Akaike Information Criterion (corrected) with partitionfinder 2 (Lanfear *et al*., 2016). Bayesian Inference (BI) analysis to infer phylogeny was carried out in mrbayes 3.6 (Ronquist & Huelsenbeck, 2003). The MCMC generations was initially set to 20 million generations with a sample frequency of 200. The stopval command was set to 0.01. Apart from the stopval command, convergence was also checked using Tracer 1.6. The burn-in frequency was set to 25%. The BI analysis was conducted on XSEDE in CIPRES Science Gateway (Miller *et al*., 2010). A Maximum Likelihood analysis under GTRGAMMA model with 1000 rapid bootstrap replicates was also performed with RAxML 8.2 (Stamatakis, 2014).

Results

Osteology

We first describe the cranial osteology of *Argyrogena fasciolata* on the basis of six crania. One of these (PUZ 322) has also been disarticulated for describing intracranial characteristics. Subsequently, the cranial osteological features of this snake has been compared to those of other genera belonging to the clade of Afrotropical, Palaearctic and Saharo-Arabian racer / whip snakes.

Cranial Osteology of *Argyrogena fasciolata* (Shaw, 1802)

Dermatocranium

Premaxilla. The edentulous premaxilla resembles a half circle when viewed from above (Fig. 1A). The posterodorsally directed ascending process is robust and subtriangular with a rounded apex. There is no nasal process. Transverse processes are broad based, short and curved backward (Fig. 1C). The triangular vomerine processes are separated by a narrow U-shaped gap. The anterior tip and the lateroventral rim of the premaxilla is somewhat 'hanging' downward.

Nasal. The nasals are paired bones consisting of a horizontal and a median vertical lamina (Fig. 1A, 2A). The anterior half of the horizontal lamina is narrow whereas the posterior half markedly expands laterally into a lateral process which bends slightly downward. The rostral ends of the horizontal laminae diverge slightly from each other, thus leaving a V-shaped space between their tips. The proximal tips rest firmly on the ascending process of the premaxilla. The anterior margin of the well-developed vertical lamina shows a slight semicircular emargination. The posterior ends of the vertical laminae, which take part in forming the prokinetic joint, are robust, directed a little downward and slightly ventrolaterally expanded (Fig. 2A).

Septomaxilla. The rostral ends of the vertical laminae of the septomaxillae remain separated from the ascending process of the premaxilla by a small soft tissue filled gap. The septomaxilla widens laterally and somewhat ventrally at about its midlength (Fig. 2C and D). The dorsal surface of this expanded region is convex in shape whereas the ventral surface is concave and forms the vomeronasal cupola with the vomer. The anterolateral edge of this expanded portion gives rise to a dorsolaterally directed conchal process. Caudad to this vomeronasal cupola part, the septomaxilla narrows abruptly into a medially ascending flange (so termed by Rieppel [2007]) which is somewhat ventrally bent and bears a laterally and ventrally expanded condyle abutting the septomaxillary process from the frontal.

Vomer. The anterior processes of the vomers firmly underlap the septomaxillae but stops short of reaching the vomerine process of the premaxilla (Fig. 1C). The inverted comma shaped vomeronasal fenestra opens up ventrally. The part of the vomer enclosing the vomeronasal organ resembles an anteriorly inclined deep cup (Fig. 2B) whose open end remains covered by the 'lid' formed by the septomaxilla. The posterodorsal region of the vomer, immediately lateral to its vertical lamina, is perforated by several small foramina through which pass vomeronasal nerve branchlets (Fig. 2A). The dorsal edges of the vertical laminae of the vomers (Groombridge, 1979; interchoanal septum of Cundall & Irish [2008]) intrude between medially ascending flanges of the septomaxillae. A large foramen perforates the ventral half of the vertical lamina. The ventral edge of the vertical lamina turns somewhat laterally but does not form a horizontal lamina. There is no medial vomeronasal fenestra between this bone and the septomaxilla.

Frontal. Frontals are paired elements forming the anterior braincase (Fig. 1A and B). The lateral margin of frontal, being wide at both proximal and distal ends and narrower at the centre, looks concave in dorsal view. The suture between the frontals, however, is straight. A supraorbital ridge demarcates orbital lamina of frontal from the dorsal horizontal lamina. The orbital laminae converge toward a crest (intertrabecular crest of McDowell [2008]) on parasphenoid's cultriform process, resulting in a little clasping of the dorsal edge of that crest. The posteroventral margin of orbital lamina forms the anterior border of the optic foramen. A medial frontal pillar (Fig. 3B) descends down from anterior medial part of each frontal which fuse with the lateral frontal flange without leaving any suture. From the subolfactory part of lateral flange, an anterolaterally directed septomaxillary process (Fig. 3A and B)) projects out. The anterior surfaces of the mesial frontal flanges are a little concave for receiving the posterior ends of the nasal vertical laminae. The anterolateral surface of the frontal bears a ridge (which is a medially turned continuation of the supraorbital ridge), a concavity beneath that ridge and an anterolaterally directed process immediately below the concavity. This surface forms a complex interlocking articulation with prefrontal.

Parietal. The parietal is a single, large element constituting the roof of the braincase (Fig. 1A, B and C). The descending processes of the parietal articulate with the prootic along its posterior border and with the lateral wings of the parabasisphenoid ventrally. The posterior dorsal end of the parietal slightly overlaps the anterior edge of the supraoccipital. The dorsolateral ridges for the external adductor origin converge posteriorly toward each other but do not meet at their ends. These ridges are more pronounced in larger skulls. The levator crest is small and remains separated from a well-developed postorbital process by a small notch. Anteriorly, the descending processes turn medial to form concave postorbital laminae (which are continuous with the dorsal surface of

the bone) whose lower medial region is emarginated to form the posterior boundary of the optic foramen.

Jugal. The jugals (Fig. 1A and B; these bones, formerly known as the postorbitals [e.g. Rieppel, 1977; Cundall & Irish, 2008], were shown to be the homolog of lizards' jugal by Palci & Caldwell [2013]) are curved bones, tapering at the dorsal end and widening towards the middle portion and again tapering at the ventral free end. The dorsal half sits on the postorbital process of the parietal, its posterior margin touching the anterior end of the levator crest. This bone does not contact the frontal.

Prefrontal. The prefrontal (Fig. 1B) has well-developed lateral lamina which extends anteriorly. The lateral lamina is perforated by a small foramen (absent on left side in PUZ 322) near its base. The orbital lamina is concave to accommodate the eye and is perforated by a lachrymal foramen which is wider caudally but narrows a little as it approaches the anterior opening. The bony roof of the lachrymal canal gives rise to an anterodorsally directed small conchal process. The ventral lamina is subrectangular and has a ligamentous connection with the palatine and maxilla. There is a notch at the dorsal junction between the lateral and the orbital laminae to receive the laterally directed process from the frontal.

Maxilla. The maxilla (Fig. 1A, B, C, 4A and B) has its proximal and caudal ends bent slightly medially. The anterior tip of the maxilla does not reach the transverse process of premaxilla and is located ahead of the rostral end of the palatine. There are 14–16 maxillary teeth (lowest count given as 12 by Wall [1921]) of which the last two slightly larger teeth are separated from the others by a small 1/2 teeth socket wide diastema. Anteriormost teeth are a little smaller than the rest. The maxilla gives rise medially to a somewhat ventrally bent palatine process below the site of its association with the prefrontal. Though the palatine process is in close proximity to the maxillary process of the palatine, these two do not actually meet or overlap. At the posterior end, the maxilla expands medially into a quadrangular ectopterygoid process.

Palatine. The palatine is a slender bone supporting 8–10 teeth (the highest count given by Wall [1921] was 11), the posterior ones being a little smaller than the anterior ones. The palatine teeth are either subequal to or a little smaller than the maxillary teeth. The palatine has a triangular maxillary process whose lateral apex is somewhat posteriorly directed. The maxillary nerve (the maxillary branch of the trigeminal nerve) canal perforates and passes through the base of this process. Behind this process, the dorsal surface of the palatine gives rise to a choanal process with a medially curved dorsal tip. The thin caudal end of the palatine overlaps the proximal end of the pterygoid.

Pterygoid. The anterior end of pterygoid underlaps the palatine; however, the proximal end of the former has a small notch within which fits a V-shaped ridge situated on the ventral surface of the palatine. The pterygoid teeth are very small and run along the medial side of the bone. There are 12–15 teeth (the upper limit given by Wilson [1967] is 17) and the teeth row does not extend behind the level of the posterior end of the ectopterygoid. The pterygoid expands into a weakly developed mesial transverse process (Fig. 4A and B) (in terms of Rieppel [1978]) below the basipterygoid ridge. A weak ridge is present on the dorsal surface of the quadrate ramus of the pterygoid. The distal end of this bone takes a lateral turn and then tapers off.

Ectopterygoid. The ectopterygoid extends from pterygoid to the maxilla (Fig. 4A). The posterior two thirds of this bone are slender. It articulates to the pterygoid by overlapping the latter. The widened anterior end overlaps the caudal end of the maxilla. The extent of emargination at the anterior end is intraspecifically variable – being of an almost truncated appearance in PUZ 322 to slightly but distinctly emarginated in the crania of the others.

Supratemporal. This compressed bone is located above the trigeminal foramina and the fenestra ovalis, on the posterior lateral wall of the prootic (Fig. 1A and C). Its anterior end does not extend beyond the prootic. Nearly one third of its posterior end projects back beyond the braincase. This section is lower in height than the anterior and middle part. The caudal end also curves slightly medially. More than half of the articulation surface with the quadrate is situated posterior to the braincase. While we followed Cundall & Irish (2008) in identifying this

→ **Fig. 1.** Dorsal (A), lateral (B) and ventral (C) views of skull (PUZ 322) and lateral (D) and medial (E) views of mandible of *Argyrogena fasciolata*. Abbreviations: Ad.Pa, adductor ridge; Ad.Qa, adductor crest on quadrate; Ang, angular; Ant.L.F, anterior labial foramen; Ar, articular; Bo, basioccipital; Ch.F, chorda tympani foramen; Ch.Pl, choanal process of palatine; Ch.Sm, conchal process of septomaxilla; Clt.Ps, cultriform process of parasphenoid; Dn, dentary; Ec, ectopterygoid; Ec.Mx, ectopterygoid process of maxilla; Eo, exoccipital; Ex.M.F, external mental foramen; Fr, frontal; Jg.Fm, jugular foramen; Ju, jugal; La, lachrymal foramen; La.Pf, lateral lamina of prefrontal; Ls, laterosphenoid; Lv, levator crest; McG, meckelian groove; Mst.Pt, mesial transverse process of pterygoid; Mx, maxilla; Mx.Pl, maxillary process of palatine; Na, nasal; Oc, occipital condyle; OpF, optic foramen; Or.Fr, orbital lamina of frontal; Or.Pf, orbital lamina of prefrontal; Pa, parietal; PBs, parabasisphenoid; Pf, prefrontal; Pl, palatine; Pl.Mx, palatine process of maxilla; Pm, premaxilla; Po, prootic; Po.M.F, posterior mylohyoid foramen; Pra, prearticular; Pt, pterygoid; Qa, quadrate; Qa.R.Pt, quadrate ramus of pterygoid; Rt.Pr, retroarticular process; Sm, septomaxilla; Sp, stapes; So, supraoccipital; Spl, splenial; St, supratemporal; Sur, surangular; Tr.Pm, transverse process of premaxilla; V2, anterior trigeminal foramen; V3, posterior trigeminal foramen; Vnf, vomeronasal nerve foramina; Vo, vomer; Vo.Pm, vomerine process of premaxilla; scale bar 5 mm.

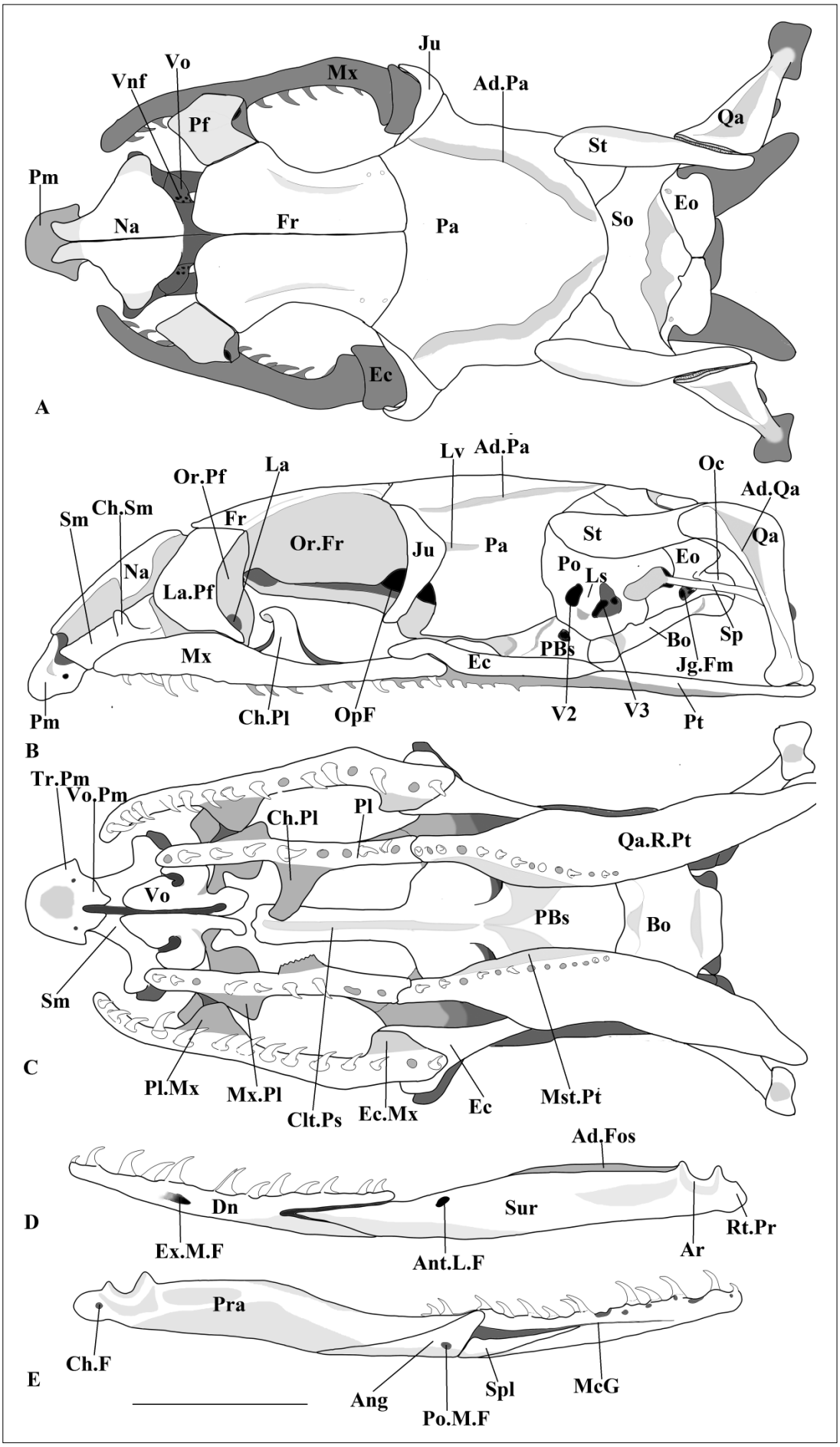
A
Ju
Vo
Vnf
Mx
Ad.Pa
Qa
Pf
St
Pm
Eo
Na
Fr
Pa
So
Ec
B
Lv
Ad.Pa
Oc
La
Or.Pf
Ad.Qa
Ch.Sm
Sm
Fr
Or.Fr
Ju
Pa
St
Qa
Na
Po
Eo
La.Pf
Ls
Sp
Bo
PBs
Mx
Ec
Jg.Fm
Pm
Ch.Pl
OpF
V2
V3
Pt
C
Tr.Pm
Vo.Pm
Ch.Pl
Pl
Qa.R.Pt
Vo
PBs
Bo
Sm
Pl.Mx
Mx.Pl
Clt.Ps
Ec.Mx
Ec
Mst.Pt
D
Ad.Fos
Dn
Sur
Rt.Pr
Ex.M.F
Ant.L.F
Ar
E
Pra
Ch.F
Ang
Spl
McG
Po.M.F

bone as a supratemporal, we note that different homology hypotheses for this bone were proposed by different authors (e.g. McDowell 2008; Warneburg & Sanchez-Villagra 2015).

Compound bone. This bone, together with the dentary, forms the mandible (Fig. 1D and E). This bone is composed of the dermatocranial surangular, prearticular and the splanchnocranial articular which are fused to each other without leaving any suture. The articular is strongly concave in order to receive the mandibular condyle of the quadrate. The anterior dorsal end of the articular is a little bilaterally flared. The medially turned retroarticular process is somewhat smaller that the articular and bears a chorda tympani foramen on its medial surface, immediately behind the articular. The medial prearticular and lateral surangular crests border the well-developed (occupying nearly half of the compound bone) mandibular or adductor fossa. An anterior labial foramen is situated on the dorsolateral edge of the compound bone, rostrad to the fossa. The alveolar canal runs through the compound bone. The dorsolateral edge of the anterior end of this bone is pointed and wedged between the posterior dorsal and ventral processes of the dentary.

Dentary. The dentary (Fig. 1D and E) bears 15 – 16 teeth (14-18 according to Wilson [1967]). The anteriormost teeth are the smallest. The teeth immediately behind the anteriormost ones are the largest and progressively become smaller posteriorly. The posterior dorsal dentigerous process extends posteriorly more than its ventral edentulous counterpart. The rostral end of dentary is rather medially turned. The meckelian canal is open along the medial surface of the dentary and stops about four teeth short of the rostral tip of this bone. The external mental foramen is situated on the lateral surface of dentary, about half way between the anterior ends of it and the compound bone (which is wedged between the posterior dorsal and ventral processes of the dentary).

Angular. This is an elongated triangular bone which is situated medial to the rostral end of the compound bone (Fig. 1E). A posterior mylohyoid foramen perforates this bone. The anterior end contacts the splenial.

Splenial. The splenial is elongated and triangular. It is articulated on the medial side of the dentary (Fig. 1E). The bone is not perforated by mylohyoid foramen.

Chondrocranium

Parabasisphenoid. The parabasisphenoid is a fusion between the anterior dermatocranial parasphenoid and posterior chondrocranial basisphenoid. The posterior half of this bone is shield like (Fig. 5A) and the widest part of the lateral wing is situated between the trijunction point of the parietal, prootic and parabasisphenoid. From the widest point of the lateral wing a basipterygoid ridge (it is more of a ridge than a process) originates and proceeds toward the midline and upon turning rostrad subsides into the basisphenoid. This ridge is less pronounced in smaller skulls. The posterior vidian canal perforates the basisphenoid near its posterior lateral corner (Fig. 5A). This runs through the bone as a closed canal and opens through a primary anterior opening (as defined by Rieppel [1979]), piercing the basipterygoid ridge. The dorsal surface bears a deeply concave pituitary fossa and the dorsum sellae somewhat overhangs the fossa (Fig. 5B). The abducens nerve foramen passes through the crista sellaris caudad and laterad to the fossa. The anterior end of the parabasisphenoid is drawn into a narrow cultriform process which does not expand anteriorly nor is its proximal end emarginated. A longitudinal, shallow concavity or groove runs along the ventral surface of this process. On the dorsal surface there is a pronounced ridge, the intertrabecular crest (Fig. 5B), which terminates rostrally by an emargination. The parabasisphenoid forms the lower boundary of the optic foramen. Below the optic foramen, the parabasisphenoid suddenly expands laterally and also slightly ventrally into a suborbital flange on each side (Fig. 3B and 5B).

Prootic. The prootic is situated caudad to the lateral wall of the parietal and rostrad to the exoccipital. It is bound ventrally by the basisphenoid and the basioccipital whereas dorsally it meets the supraoccipital. There is a large aperture – trigeminofacialis chamber – on the medial surface of prootic which gets divided into anterior and posterior trigeminal foramina (Fig. 1B and 5C) by a laterosphenoid as the chamber opens on the lateral surface. The laterosphenoid is laterally convex whereas the region immediately below it abruptly becomes concave and is perforated by a small foramen. The hyomandibular nerve foramen opens within posterior trigeminal foramen. There is a very small foramen below the anterior trigeminal foramen. Immediately below the surface for articulation with the supratemporal there is a small horizontal tuberosity which acts as a supporting shelf for the anterior end of the supratemporal. The posterior border of prootic is deeply emarginated to form the anterior margin of the fenestra ovalis. The prootic also partly contributes to the crista circumfenestralis dorsalis which surrounds the fenestra ovalis dorsally.

Exoccipital. The exoccipitals form the posterior dorsal margin of the cranium. The exoccipitals also contribute partly to the crista circumfenestralis dorsalis. The crista circumfenestralis ventralis, which surrounds the fenestra ovalis ventrally, is formed entirely by the exoccipital. The stapedial shelf of the crista interfenestralis demarcates a more posteroventral apertura lateralis for recessus scalae tympani (Fig. 5C). The crista interfenestralis expands into a small tuberosity below the juxtastapedial recess which abuts ventrally a similar convexity from the basioccipital. The jugular foramen is situated behind the juxtastapedial recess and is separated from the latter by a bony strut (Fig. 1B and 5C). Within the jugular foramen, there are three are foramina opening – one large anterior foramen for the vagus nerve and two small pos-

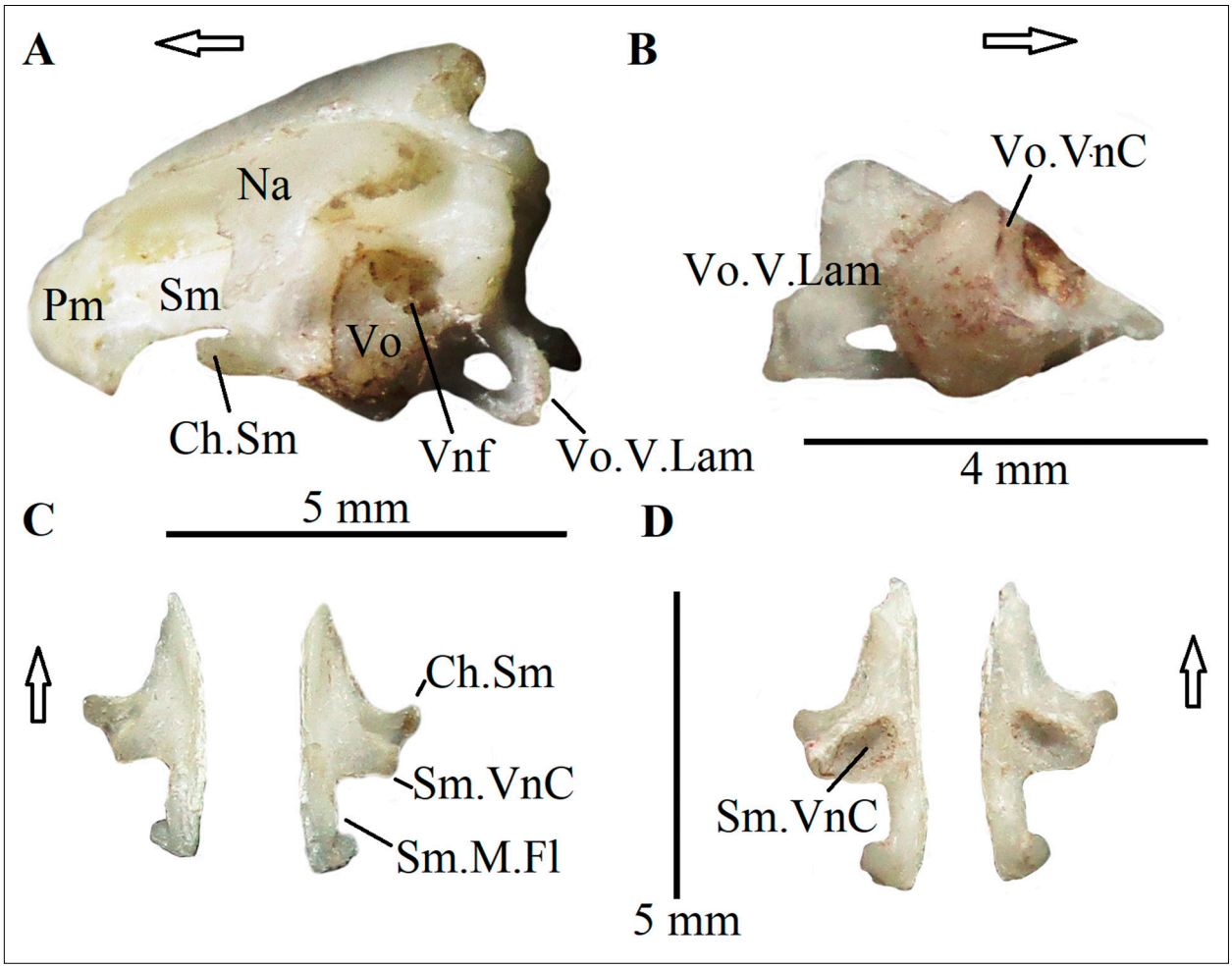

Fig. 2. Snout bones of *Argyrogena fasciolata* (PUZ 322). A. Posterolateral view of snout; B. lateral view of right vomer; C. dorsal surface of septomaxilla; D. ventral surface of septomaxilla. Arrows indicate the anterior end. Abbreviations: Sm.M.FL, medially ascending flange of septomaxialla; SmVnc, vomeronasal cupola part of septomaxilla; Vo.V.Lm, vertical lamina of vomer; Vo.Vnc, vomeronasal cupola part of vomer; see legend of Fig. 1 for the rest of the abbreviations.

terior foramina, situated one above the other (these two may act as passageways for the hypoglossal nerve; two similar foramina in *Boaedon virgatus* were described as such by McDowell [1987]). Caudad to jugular foramen the exoccipital expands into a small posteriorly directed triangular process. Above this process is a small triangular paroccipital expansion. A small foramen is present behind this paroccipital process. The exoccipitals contribute laterally to the occipital condyle.

Supraoccipital. The supraoccipital (Fig. 1A) is a single bone between the parietal and exoccipital. The posterior border looks like a curly bracket with its closed end facing the caudal end of the braincase. A strong transverse crest is present across this bone.

Splanchnocranium

Quadrate. This is an elongated, triangular bone (Fig. 1B) from which the mandible remains suspended. The cephalic condyle, the dorsalmost part articulating with the supratemporal, is well-developed and somewhat pointed anteriorly. Along the anterolateral edge of the bone runs an adductor crest. The mandibular condyle is heterocoelous. There is a concavity immediately above the mandibular condyle, on the anterior surface of the bone. There is a small foramen opening within this concavity. The ovoid articulatory facet for the stapes is situated on the medial surface of the quadrate, at about the midheight position of the bone.

Stapes. The stapes is a very slender, elongated bone (Fig. 1B and 5A) with a small rounded footplate. The stapes, in its natural articulated position, is somewhat posteroventrally slanted to meet the articulatory facet on the quadrate (though the contact is mainly established through soft tissue).

Comparison of the cranial osteological features

The cranial features of *Argyrogena fasciolata* is compared here with those of all other genera forming the clade of Afrotropical, Palaearctic and Saharo-Arabian

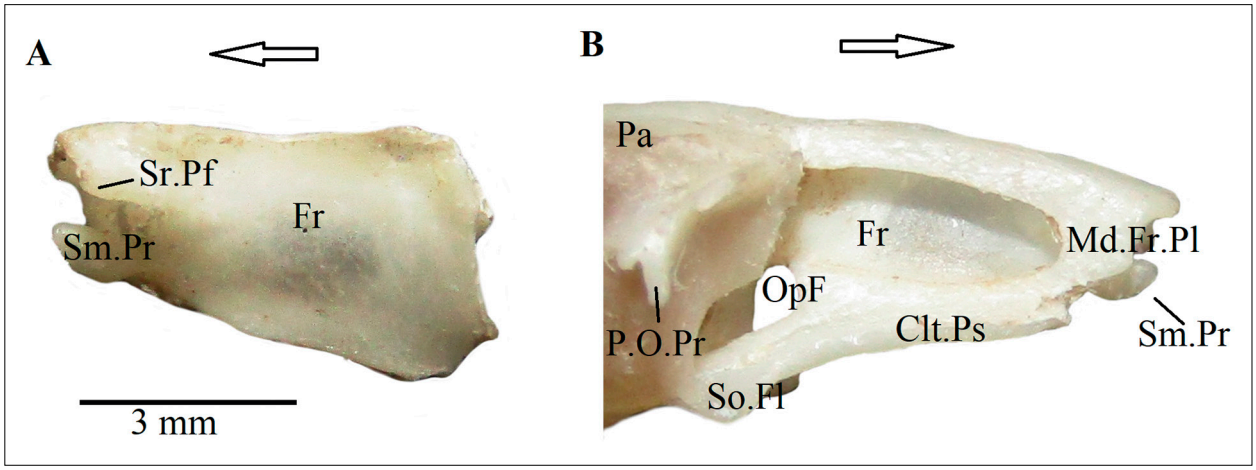

Fig. 3. Frontal bones of *Argyrogena fasciolata* (PUZ 322). A. lateral view; B. medial view after removal of the right frontal. Arrows indicate the anterior end. Abbreviations: Md.Fr.Pl, medial frontal pillar; P.O.Pr, postorbital process of parietal, visible after removal of jugal; Sr.Pf, surface for prefrontal articulation; Sm.Pr, septomaxillary process; So.Fl, suborbital flange; see legend of Fig. 1 for the rest of the abbreviations.

racer / whip snakes in the phylogenies inferred by Pyron *et al*. (2013) and Figueroa *et al*. (2016) (We would like to note here that the aforesaid clade was not monophyletic in our molecular phylogenetic analyses (see the next section) but this most probably reflects the need for more data to resolve the deeper level relationships of this clade rather than its non-monophyly).

Argyrogena fasciolata differs from *Platyceps*, the genus which is said to approach the former taxon very closely in external morphology (Wilson, 1967), in possessing a backwardly curved transverse process (vs. laterally directed, narrow transverse process in *Platyceps* [Szunyoghy, 1932; present study]), an elongated nasal horizontal lamina (vs. shorter nasal in *Platyceps*; however, the basic shape of the nasal horizontal lamina of *Platyceps* and *Argyrogena* is similar – concave anterior and convex posterior margins [when seen from above] of the lateral expansion of the horizontal lamina [Szunyoghy, 1932; present study]) and a mesial transverse process of the pterygoid (vs. no such mesial expansion of the pterygoid in *Platyceps*).

The three characters which distinguish *Argyrogena fasciolata* from *Platyceps* serves to distinguish the former also from *Dolichophis*, *Eirenis*, *Hierophis*, *Hemorrhois*, *Hemerophis*, *Orientocoluber* and *Spalerosophis* (Phisalix, 1922; Szunyoghy, 1932; Schätti & Utiger, 2001; Mahlow *et al*., 2013; Sadeghi *et al*., 2014; present study). *A. fasciolata* can be further diagnosed from *Hierophis* and *Orientocoluber* by having a nasal dominated prokinetic joint (vs. nasal playing a minor if any role in forming the prokinetic joint; this character may hold true for other genera mentioned above [except for *Platyceps* and probably also *Spalerosophis*] but this requires a thorough study). The emarginated proximal end of the ectopterygoid of *A. fasciolata* serves to distinguish it from *Dolichophis*, *Eirenis*, *Hierophis* and *Orientocoluber* (in *Dolichophis* the anterior lateral process is elongated [Szunyoghy, 1932] whereas in other genera the anterior end of ectopterygoid is deeply forked to produce anterior lateral and medial processes; see McDowell [1986] for a definition of those character states). The cultriform process of the parasphenoid is more or less the same width throughout its length and without any emargination at the proximal end in *Argyrogena* whereas in *Dolichophis*, *Eirenis*, *Hierophis*, *Hemorrhois*, *Hemerophis*, *Orientocoluber*, *Platyceps collaris* and *Platyceps rhodorachis* (but not so in other *Platyceps* spp. examined by us) the cultriform process expands towards the anterior end and is strongly emarginated (not emarginated in *Hierophis viridiflavus*) (Szunyoghy, 1932; Schätti, 1987; Schätti & Utiger, 2001; present study). There is a lack of distinct diastema in the maxillary dentition which further distinguishes *Spalerosophis* from *Argyrogena* (Smith, 1943; present study).

Argyrogena fasciolata is separable from *Rhynchocalamus* and *Muhtarophis*, whose skull has been described by Avci *et al*. (2015), in the following ways; the anterior end of the maxilla is located well in front of the prefrontal (vs. the proximal end of maxilla is situated below the prefrontal in both *Rhynchocalamus* and *Muhtarophis*), possesses higher number of maxillary (12 – 16) and palatine teeth (8 – 11) (vs. less than 8 maxillary and 5 palatine teeth in *Rhynchocalamus* and *Muhtarophis*), mesial transverse process on pterygoid (vs. no such process in *Rhynchocalamus* and *Muhtarophis*), mandibular teeth (vs. less than 10 teeth in *Rhynchocalamus* and *Muhtarophis*), a supratemporal-quadrate articulation that extend beyond the exoccipital (vs. this articulation does not extend beyond the exoccipital in the latter two genera) and a narrow cultriform process (vs. a wide process in both *Rhynchocalamus* and *Muhtarophis*). *A. fasciolata* further differs from *Rhynchocalamus* in having an ascending process of the premaxilla (vs. no ascending process in *Rhynchocalamus*, well-developed jugal (vs. a very small one in the latter) and a teeth bearing pterygoid (vs. edentulous pterygoid in *Rhynchocalamus*).

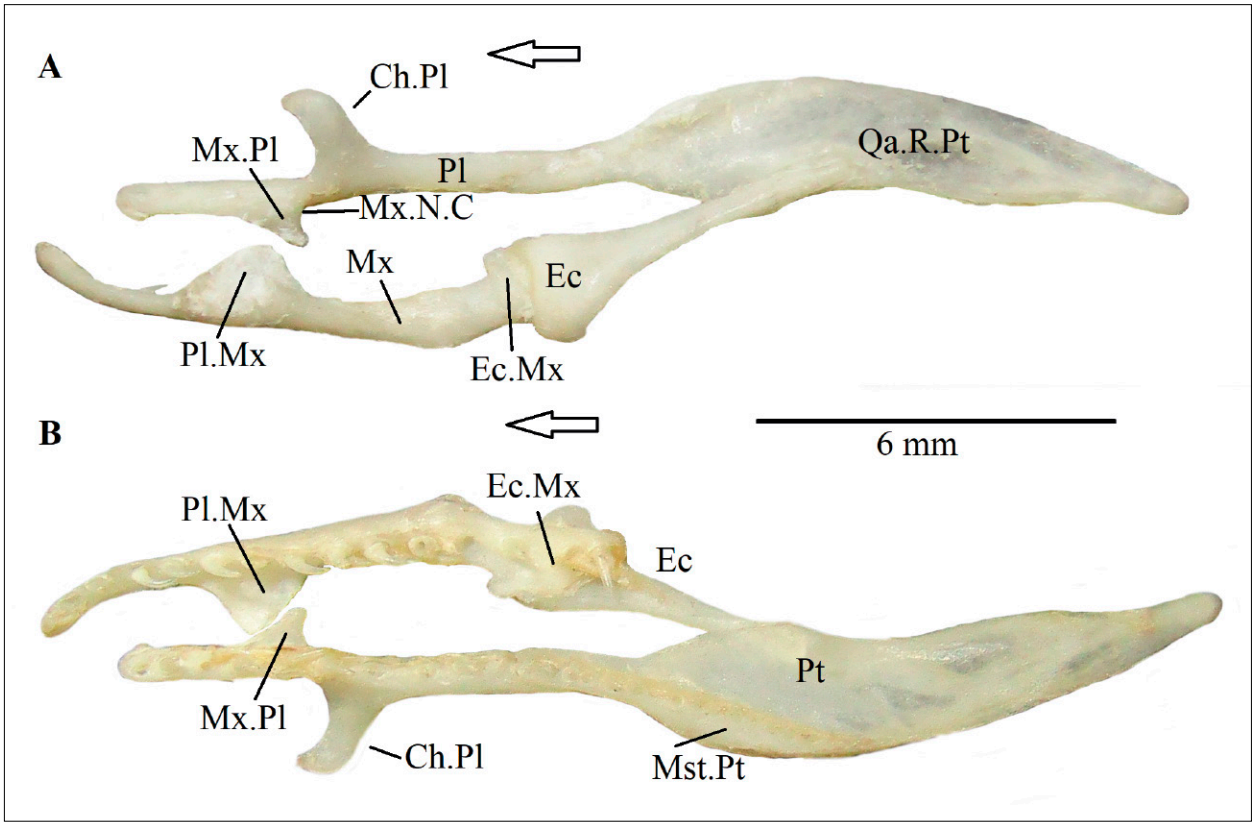

Fig. 4. Palatomaxillary arch bones of *Argyrogena fasciolata* (PUZ 322). A. dorsal view of palatomaxillary arch; B. ventral view of the palatomaxillary arch; Arrows indicate the anterior end. Abbreviations: Mx.N.C, maxillary nerve canal; see legend of Fig. 1 for the rest of the abbreviations.

Argyrogena fasciolata is distinguished from *Mopanveldophis zebrinus* in having a lower number of maxillary teeth (the maximum number of maxillary teeth known to occur in the former is 16 whereas in the latter it is 19) (Broadley & Schätti, 2000). Other cranial osteological characteristics of the monotypic genus *Mopanveldophis* are unknown.

Another monotypic genus *Bamanophis* containing a single species *B. dorri* is distinguishable from *Argyrogena fasciolata* in possessing a slightly higher number of maxillary teeth (15–19) (Schätti & Trape, 2008), a rounded palatine process of the maxilla (Chippaux, 2006; Schätti & Trape, 2008) (vs. a distinctly triangular process in *A. fasciolata*) and a cultriform process of the parasphenoid with an expanded and emarginated proximal end (Fig. 3 of Schätti & Trape [2008]).

Macroprotodon spp. are characterized by having a maxilla with 6 teeth followed by a diastema, 2–5 smaller teeth and finally 2 rear fangs (Wade, 2001; Geniez, 2018) and these dentitional characteristics help to distinguish members of this genus from *Argyrogena fasciolata*. Other characters pertaining to the cranium of *Macroprotodon* are not known.

Lytorhynchus is distinguishable from *Argyrogena* in that the former possesses a cruciform premaxilla, only 6–9 teeth on the maxilla (Smith, 1943; present study), poorly developed lateral lamina of the prefrontal (vs. well-developed lateral lamina with an anteriorly directed apex in *A. fasciolata*), a supratemporal-quadrate articulation that does not extend beyond the exoccipital caudally and lacks any mesial transverse process of pterygoid.

Presence of 9 teeth on the maxilla of *Wallaceophis gujaratensis* (Mirza *et al*., 2016) distinguishes this species from *Argyrogena fasciolata*. Apart from maxillary and palatine dentition, no other information on cranial osteology is available for *W. gujaratensis*. Cranial osteology *Wallophis brachyura* – the sister taxon of *W. gujaratensis* (Mirza & Patel, 2018) – remains unknown barring its maxillary dentition (Smith, 1943) which does not effectively diagnose it from *A. fasciolata*.

The comparison presented above shows that among those genera for which complete, near complete or at least considerable amount of osteological data are available (namely *Dolichophis*, *Eirenis*, *Hierophis*, *Hemorrhois*, *Muhtarophis*, *Orientocoluber*, *Platyceps*, *Rhynchocalamus* and *Spalerosophis*), it is *Platyceps* which is the least dissimilar to *Argyrogena*. In the phylogeny (Fig. 6; also see the next section) inferred from molecular data, *A. fasciolata* is sister to all other *Platyceps* spp. However, we cannot find any unambiguous synapomorphy in cranial characters supporting the sister relationship between *Argyrogena* and *Platyceps* apart from the overall phenetic similarities. Mesial transverse process of the ectopterygoid appears to be an autapomorphy of *A. fasciolata*.

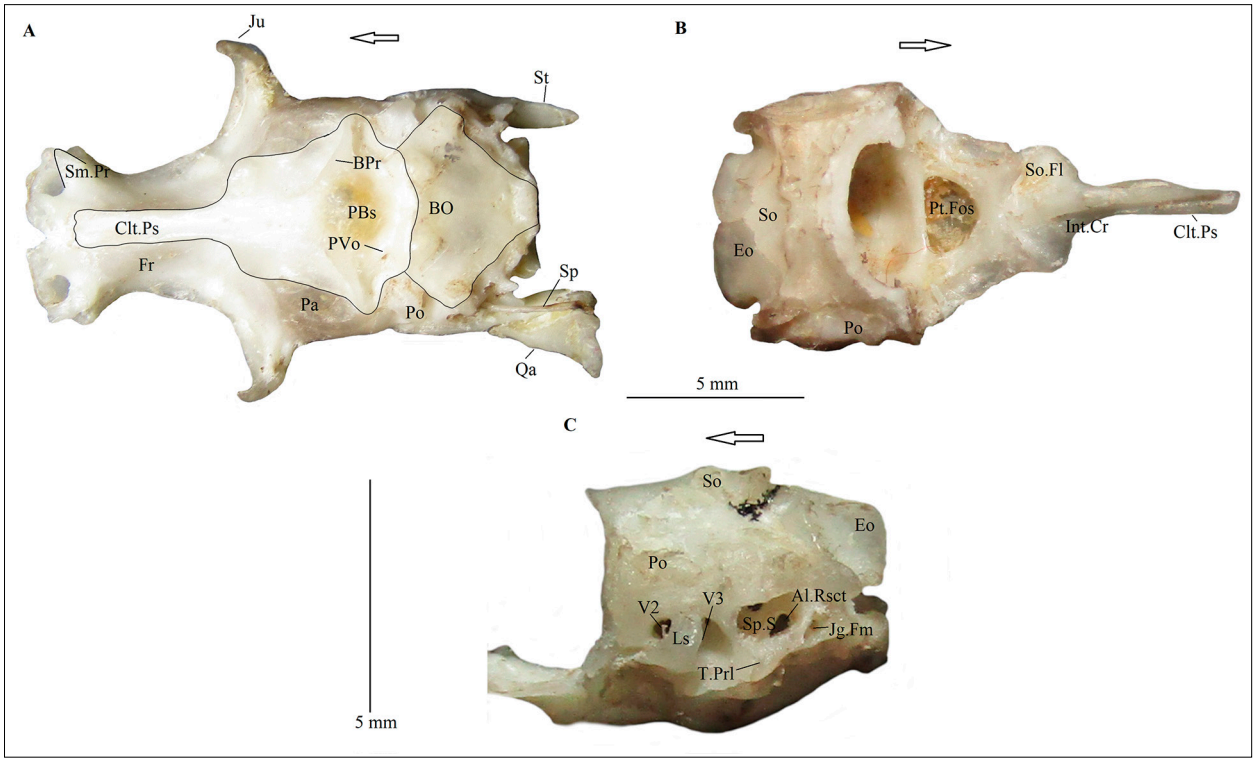

Fig. 5. Chondrocranial bones of the cranium of *Argyrogena fasciolata* (PUZ 322). A. ventral view of braincase showing parabasisphenoid and basioccipital (outlined in black); B. dorsal view of parabasisphenoid; C. lateral view of otic region (crista circumfenestralis cut away); Arrows indicate the anterior end. Abbreviations: Al.Rsct, apertura lateralis of recessus scalae tympani; BPr, basipterygoid ridge; PVo, posterior vidian canal opening; Int.Cr, intertrabecular crest; Pt.Fos, pituitary fossa; Sp.S, stapedial shelf; Tr.PrI, tuberosity of processus interfenestralis. see legend of Fig. 1 for the rest of the abbreviations.

Phylogeny

The Bayesian Inference analysis hit the inbuilt convergence diagnostics (i.e. value of average standard deviation of split frequencies below 0.01) after 13.94 million generations. In the BI tree (Fig. 6) *Argyrogena fasciolata* is recovered as basal to *Platyceps* spp. with moderate support (posterior probability 0.82).

The Maximum Likelihood analysis (lnL = –14342.5) returned a phylogenetic tree (not shown) which is mostly identical with the BI topology. *Argyrogena fasciolata* is again recovered as sister to *Platyceps* spp., though bootstrap support was somewhat low (52 %).
Arygyrogena + *Platyceps* spp. belongs to a clade of medium to large sized Afrotropical, Palaearctic and Saharo-Arabian racers, diadem snakes and whip snakes belonging to genera, apart from the two aforementioned ones, *Spalerosophis* and *Hemorrhois*. This clade was also recovered in other works (e.g. Schätti & Utiger 2001; Nagy *et al*. 2004; Utiger *et al*. 2005), albeit without *A. fasciolata*.

The clade of Afrotropical, Palaearctic and Saharo-Arabian snakes was not recovered to be monophyletic with respect to the Oriental rat and trinket snakes (genera *Coelognathus*, *Elaphe* and *Ptyas*); this, however, indicates a need to incorporate more loci, preferably nuclear ones, into the analysis. However, the subclade to which *Argyrogena fasciolata* belongs to shows relationships consistent with those demonstrated in other studies as has already been mentioned.

Generic systematics of *Argyrogena fasciolata* (Shaw, 1802)

George Shaw described this species as *Coluber fasciolatus* on the basis of a plate by Patrick Russell. Two more nomina, namely *Coluber hebe* Daudin, 1803 and *Coluber curvirostris* Cantor, 1839, were synonymized with *Coluber fasciolatus* by Günther (1864) who assigned the species to *Zamenis*. Cope (1862) was most probably the first to suspect that the affinity of this species lies with palaearctic racers or whip snakes as can be deduced from his usage of the generic epithet *Tyria* Fitzinger, 1826 (this was preoccupied by *Tyria* Hübner, 1819, a lepidopteran genus, and therefore a homonym). Günther (1864) was the first to explicitly express that this snake is closely related to the racers of the 'Mediterranean genus' – *Zamenis* in this case. He included species currently classified under the genera *Platyceps* and *Spalerosophis*, apart from *C. fasciolatus*, in *Zamenis* in his 1864 contribution on herpetofauna of British India. Boulenger (1893) placed this species under *Zamenis* but Boulenger's *Zamenis* was a polyphyletic hotchpotch of several disparate Afrotropical, Nearctic, Neotropical,

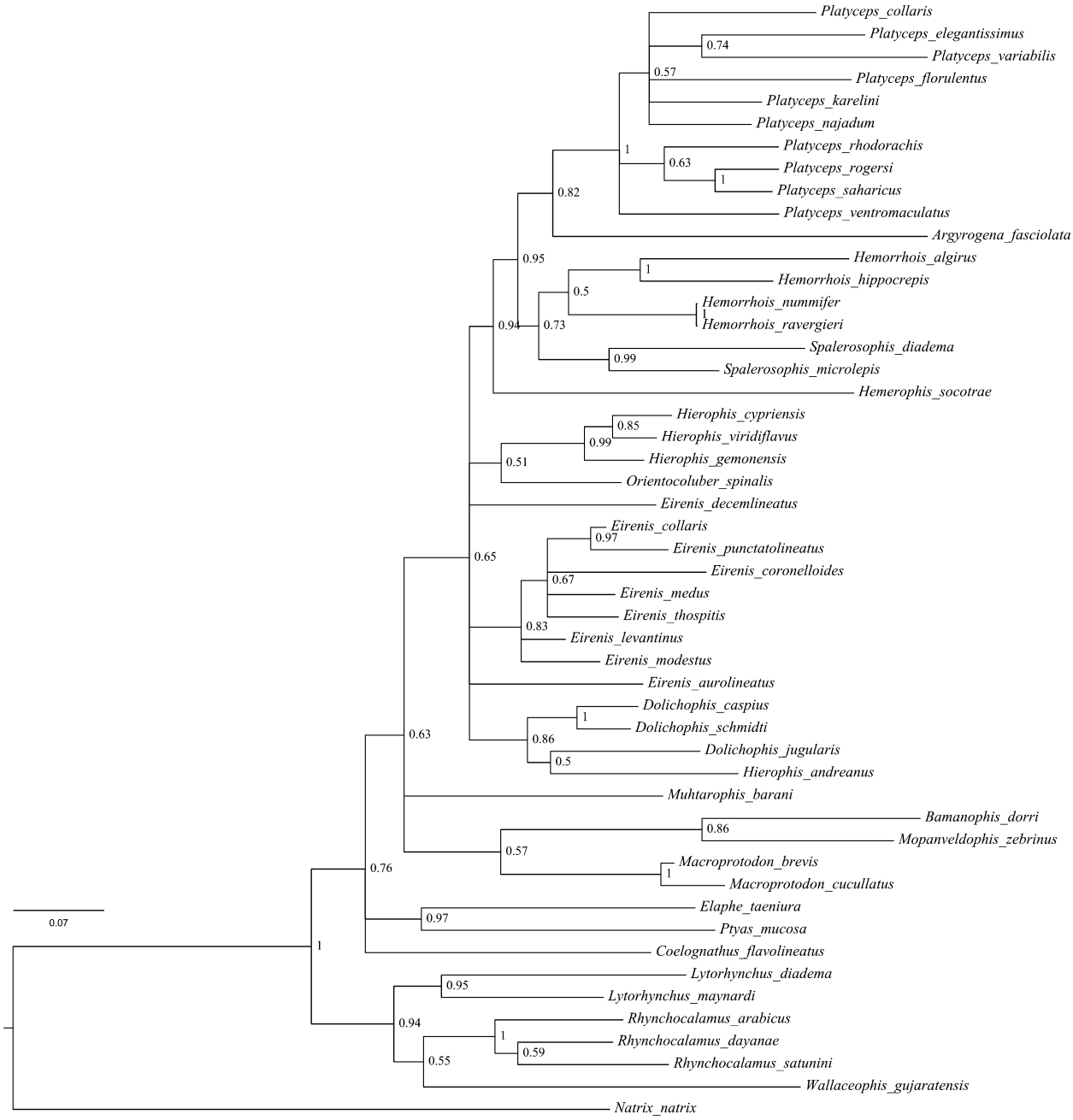

Fig. 6. Bayesian Inference phylogeny of Afrotropical, Palaearctic and Saharo-Sindian racers, including *Argyrogena fasciolata*. Values besides nodes are posterior probabilities.

Saharo-Arabian, Palaearctic and Oriental genera. For the first half of the twentieth century this species has variously been assigned to either *Zamenis* (e.g. Wall, 1924) or *Coluber* (e.g. Smith, 1943), in association with Saharo-Arabian and Palaearctic racers and whip snakes. Wilson's (1967) comparison of the morphological features of this snake with those of other species then classified under *Coluber* led him to opine that this species differs enough from others to warrant placement in a monotypic genus; therefore he revived *Argyrogena* Werner, 1924. The comparison presented by Wilson shows that *A. fasciolata* share some external morphological similarities with the species belonging to the *Platyceps* group of Inger & Clark (1943). However, neither Wilson nor workers from the pre-cladistics era presented any phylogeny with this species included. Utiger *et al*. (2005) also consider that *A. fasciolata* is a member of the clade to which the Afrotropical, Palaearctic and Saharo-Arabian racers belong, however the specific relationships of *A. fasciolata* within this clade remain unknown. Our cranial osteological comparison suggests that it is comparatively more similar to *Platyceps* than it is to any other racer genera – in fact, the skull of *A. fasciolata* is essentially a *Platyceps* skull with fossorial adaptations in the bones of the snout and the prokinetic joint. The phylogenies inferred for the present study from mitochondrial DNA

data also recovers *Argyrogena* as basal to other *Platyceps*. Together *A. fasciolata* and *Platyceps* spp. form a monophyletic clade and hence the former can be assigned to *Platyceps* (in which case the specific epithet should be spelt as *fasciolatus*), thus making the former genus more inclusive. Some systematists (e.g. Platnick, 1976; Avci *et al*., 2015) object to the use of monotypic genera from a cladistic point of view with which we concur. However, as has already been stated in the Introduction for the last four decades most systematists have followed Wilson's arrangement. Furthermore, it is not nested within *Platyceps* and thus does not render the latter paraphyletic. Therefore, we keep the species under discussion in *Argyrogena* to maintain stability, in keeping with the spirit of the ICZN general recommendations (Appendix B of the Code, fourth version [ICZN, 1999]).

Discussion

As Bell & Mead (2014) discussed, a shortcoming observed in many studies on squamate osteology is that these studies are based on very few (often only one or two) specimens. The present study attempts to overcome this by studying as many skulls of *Argyrogena fasciolata* as can be accessed. Our study on six skulls shows the presence of intraspecific variation in the shape of the anterior end of the ectopterygoid and variation in the number of teeth. Variations observed in adductor ridges on the parietal and basipterygoid ridges on the parabasisphenoid seems to be related to the age of the individuals as these are more pronounced in the skulls of individuals of larger size. Previously Wilson (1967) commented upon fossorial adaptations in the premaxilla, nasal and countersunk lower jaw of this snake. We note here that the prokinetic joint is dominated by the nasal rather than the septomaxilla which is more common in colubrids (Rieppel, 2007; Cundall & Irish, 2008); the nasals make contact with almost the entire height of the mesial frontal pillars, thus making a strong nasofrontal joint. This type of prokinetic joint characterizes fossorial snakes (Rieppel, 2007) and *A. fasciolata* is known to have much more of a predilection for a semifossorial mode of life (Minton, 1966). However, the *A. fasciolata* skull is remarkable in that the cranial feature caudad to snout shows none of the common fossorial adaptations listed by Cundall & Irish (2008) for burrowing colubrid skulls. It seems possible that this snake uses its snout to poke through loose soil (Minton reports that *A. fasciolata* resides in habitats with loose soil dotted about with rodent burrows) in front of the narrow entrance of burrows in search of rodents and hence, the burrowing adaptations are limited mostly to snout region. However, observation of live snakes in their natural habitat and functional morphological studies are needed in order to elucidate just how they use their snout. Future studies can also focus on the inner ear morphology of *A. fasciolata* and related *Platyceps* spp. as the osteological features of this region were shown to be correlated, to some extent, with mode of living in snakes (Palci *et al*. 2017).

Cranial osteology suggests close relationships of *A. fasciolata* with racers of the genus *Platyceps* and this is found to be the case in the molecular phylogenies inferred. Among all the species belonging to the Afrotropical, Palaearctic and Saharo-Arabian racer / whip snake clade, this is the species which achieves the easternmost distribution, being distributed in eastern India and Bangladesh. Apart from this species, only two species belonging to genus *Playceps* – namely *Platyceps bholanathi* and *Platyceps gracilis* – extend well into the Oriental realm, being found in peninsular India (Wallach *et al*., 2014). Other species belonging to *Platyceps* are mainly distributed in Afrotropical, Saharo-Arabian and adjacent Palaearctic regions (Wallach *et al*., 2014; Geniez, 2018; Spawls *et al*., 2018). The same also applies mostly to *Spalerosophis*, *Hemerophis* and *Hemorrhois* (Chippaux, 2006; Schätti *et al*., 2009; Geniez, 2018). So, it appears that the three aforesaid realms have been the main centre of radiation of the *Platyceps-Argyrogena-Hemorrhois-Spalerosophis-Hemerophis* clade with a few short distance incursions into the Oriental realm (for instance, *Platyceps ventromaculatus* and *Spalerosophis atriceps* in northwestern India [Schätti & Schmitz, 2006]) and at least two (may be three if *P. bholanathi* and *P. gracilis* are not each others' sister; these two species have never been included in a phylogenetic analysis) instances of deep intrusion into the Orient, namely by the two species of *Platyceps* mentioned above and *A. fasciolata*.

Acknowledgements

We are deeply indebted to following persons for kindly making available high quality photographs of skeletal materials under their care available to us – Alan Resetar and Joshua Mata (FMNH), David Kizirian and Lauren Vonnahme (AMNH), Christopher Austin, Jackson Roberts and Seth Parker (LSUMNS). We also thank data editors of 'Scan All Snakes' project on MorphoSource for allowing us to download two of the micro-CT scans. We are grateful to two anonymous reviewers for their highly constructive comments which have been a great aid in improving the quality to the manuscript. Financial assistance to KP and SM by the Faculty Research and Professional Development Plan, Presidency University, is gratefully acknowledged. SD would like to express gratitude to N. N. Dutta for constant encouragement and advice. SD and SR thank Archan Pal for help in laboratory work.

References

Avci, A., Ilgaz, C., Rajabizadeh, M., Yilmaz, C., Üzüm, N., Adriaens, D., Kumlutas, Y. & Olgun, K. (2015). Molecular phylogeny and micro CT-scanning revealed extreme cryptic diversity in kukri snake, *Muhtarophis* gen. nov., a new genus

for *Rhynchocalamus barani* (Serpentes: Colubridae). *Russian Journal of Herpetology*, **22**, 159–174.

Bell, C. J. & Mead, J. I. (2014). Not enough skeletons in the closet: collections-based anatomical research in an age of conservation conscience. *The Anatomical Record*, **297**, 344–348.

Boulenger, G. A. (1890). *The fauna of British India, including Ceylon and Burma*. *Reptilia and Batrachia*. London, Taylor and Francis.

Boulenger, G. A. (1893). *Catalogue of the Snakes in the British Museum* (*Natural History*). *Volume I*. London, The Trustees (British Museum).

Broadley, D. G. & Schätti, B. (2000). A new species of *Coluber* from Namibia (Reptilia: Serpentes). *Madoqua*, **19**, 171–174.

Chippaux, J. P. (2006). *Les serpents d'Afrique occidentale et centrale*. Paris, IRD editions.

Constable, J. D. (1949). Reptiles from the Indian peninsula in the Museum of Comparative Zoology. *Bulletin of the Museum of Comparative Zoology*, **103**, 59–160.

Cope, E. D. (1862). Notes upon some reptiles of the Old World. *Proceedings of the Academy of Natural Sciences of Philadelphia*, **14**, 337–344.

Cundall, D. & Irish, F. (2008). The snake skull, pp. 349–692 *in*: Gans, C., Gaunt, A.S. & Adler, K. (eds) *Biology of the Reptilia*. Vol. 20. New York, Society for the Study of Amphibians and Reptiles.

Das, I. & Silva, A. D. (2005). *A Photographic Guide to Snakes and Other Reptiles of Sri Lanka*. London, New Holland Publishers (UK) Ltd.

Figueroa, A., Mckelvy, A.D., Grismer, L.L., Bell, C.D. & Lailvaux, S.P. (2016). A species-level phylogeny of extant snakes with description of a new colubrid subfamily and genus. *PloS ONE*, **11**, e0161070.

Fraser, A. G. L. (1937). The snakes of Deolali. With notes on their comparative osteology and peculiarities of dentition. Part III. *Journal of the Bombay Natural History Society*, **39**, 464–501.

Geniez, P. (2018). *Snake of Europe, North Africa & Middle East*. *A Photographic Guide*. New Jersey, Princeton University Press.

Groombridge, B. (1979). On the vomer in Acrochordidae (Reptilia: Serpentes), and its cladistic significance. *Journal of Zoology*, **189**, 559–567.

Günther, A. (1858). *Catalogue of Colubrine Snakes in the Collection of the British Museum*. London, The Trustees (British Museum).

Günther, A. C. L. G. (1864). *The reptiles of British India*. London, Ray Society.

Holt, B. G., Lessard, J., Borregaard, M. K., Fritz, S. A., Araujo, M. B., Dimitrov, D., Fabre, P., Graham, C. H., Graves, G. R., Jønsson, K. A., Nogués-Bravo, D., Wang, Z., Whittaker, R. J., Fjeldså, J. & Rahbek, C. (2012). An update of Wallace's zoogeographic regions of the world. *Science*, **339**, 74–78.

Inger, R. F. & Clark, P. J. (1943). Partition of the genus *Coluber*. *Copeia*, **1943**, 141–145.

International Commission on Zoological Nomenclature (ICZN) (1999). *International Code of Zoological Nomenclature, 4th edition*. London, The International Trust for Zoological Nomenclature.

Khedkar, T., Sharma, R., Tiknaik, A., Khedkar, G., Naikwade, B. S., Ron, T. B. & Haymer, D. (2015). DNA barcoding using skin exuviates can improve identification and biodiversity studies of snakes. *Mitochondrial DNA*, **27**, 499–507.

Kumar, S., Stecher, G., Li, M., Knyaz, C. & Tamura, K. (2018). MEGA X: Molecular evolutionary genetics analysis across computing platforms. *Molecular Biology and Evolution*, **35**, 1547–1549.

Lanfear, R., Frandsen, P. B., Wright, A. M., Senfeld, T., Calcott, B. (2016). partitionfinder 2: new methods for selecting partitioned models of evolution for molecular and morphological phylogenetic analyses. *Molecular Biology and Evolution*, **34**, 772–773.

Mahlow, K., Tillack, F., Schmidtler, J. F. & Müller, J. (2013). An annotated checklist, description and key to the dwarf snakes of the genus *Eirenis* Jan, 1863(Reptilia: Squamata: Colubridae), with special emphasis on the dentition. *Vertebrate Zoology*, **63**, 41–85.

Mcdowell, S. B. (1986). The architecture of the corner of the mouth of colubroid snakes. *Journal of Herpetology*, **20**, 353–407.

Mcdowell, S. B. (1987). Systematics, pp. 3–50 *in*: Seigel, S. A., Collins, J. T. & Novak, S. S. (eds) *Snakes – Ecology and Evolutionary Biology*. New York, McGraw-Hill Publishing Company.

Mcdowell, S. B. (2008). The skull of Serpentes, pp. 467–620 *in*: Gans, C., Gaunt, A. S. & Adler, K. (eds) *Biology of the Reptilia*. Vol. 21. New York, Society for the Study of Amphibians and Reptiles.

Mertens, R. (1969). Die Amphibien und Reptilien West-Pakistans. *Stuttgarter Beiträge zur Naturkunde*, **197**, 1–96.

Miller, M. A., Pfeiffer, W. & Schwartz, T. (2010). Creating the CIPRES Science Gateway for inference of large phylogenetic trees. *Proceedings of the Gateway Computing Environments Workshop* (*GCE*), 1–8.

Minton, S. A. (1966). A contribution to the herpetology of west Pakistan. *Bulletin of the American Museum of Natural History*, **134**, 27–184.

Mirza, Z. A., Vyas, R., Patel, H., Meheta, J. & Sanap, R. V. (2015). A new Miocene-divergent lineage of old world racer snake from India. *PLoS ONE*, **11**, e0154301.

Mirza, Z. A. & Patel, H. (2018). Back from the dead! Resurrection and revalidation of the Indian endemic snake genus *Wallophis* Werner, 1929 (Squamata: Colubridae) insights from molecular data. *Mitochondrial DNA Part A*, **29**, 331–334.

Nagy, Z. T., Lawson, R., Joger, U. & Wink, M. (2004). Molecular systematics of racers, whipsnakes and relatives (Reptilia: Colubridae) using mitochondrial and nuclear markers. *Journal of Zoological Systematics and Evolutionary Research*, **42**, 223–233.

Palci, A. & Caldwell, M. W. (2013). Primary homologies of the circumorbital bones of snakes. *Journal of Morphology*, **274**, 973–986.

Palci, A., Hutchinson, M. N., Caldwell, M. W. & Lee, M. S. Y. (2017). The morphology of the inner ear of squamate reptiles and its bearing on the origin of snakes. *Royal Society Open Science*, **4**, 170685.

Phisalix, M. (1922). *Animaux venimeux et venins*. Paris, Masson & C Editeurs.

Platnick, N. I. (1976). Are monotypic genera possible? *Systematic Zoology*, **25**, 198–199.

Pyron, R. A., Burbrink, F. T. & Wiens, J. J. (2013). A phylogeny and revised classification of Squamata, including 4161 species of lizards and snakes. *BMC Evolutionary Biology*, **13**, 1–53.

Ratnasingham, S. & Hebert, P. D. N. (2007). BOLD: the Barcode of Life Data system. *Molecular Ecology Notes*, **7**, 355–364.

Rieppel, O. (1977). Studies on the skull of the Henophidia (Reptilia:Serpentes). *Journal of Zoology*, **181**, 145–173.

Rieppel, O. (1978). A functional and phylogenetic interpretation of the skull of the Erycinae (Reptilia, Serpentes). *Journal of Zoology*, **186**, 185–208.

Rieppel, O. (1979). The evolution of the basicranium in the Henophidia (Reptilia: Serpentes). *Zoological Journal of the Linnean Society*, **66**, 411–481.

Rieppel, O. (2007). The naso-frontal joint in snakes as revealed by high-resolution X-ray computed tomography of intact and complete skulls. *Zoologischer Anzeiger*, **246**, 177–191.

Ronquist, F. & Huelsenbeck, J. P. (2003). mrbayes 3: Bayesian phylogenetic inference under mixed models. *Bioinformatics*, **19**, 1572–1574.

Sadeghi, N., Hosseinian, S. S. Y., Rastegar-Pouyani, N. & Rajabizadeh, M. (2014). Skull comparison between *Eirenis collaris* and *Dolichophis jugularis* (Serpentes: Colubridae) from Iran. *Iranian Journal of Animal Biosystematics*, **10**, 87–100.

Schätti, B. (1987). The Phylogenetic significance of morphological characters in the Holarctic racers of the genus *Coluber* Linnaeus, 1758 (Reptilia, Serpentes). *Amphibia-Reptilia*, **8**, 401–418.

Schätti, B. & Utiger, U. (2001). *Hemerophis*, a new genus for *Zamenis socotrae* Günther, and a contribution to the phylogeny of Old World racers, whip snakes and related genera (Reptilia: Squamata: Colubrinae). *Revue Suisse de Zoologie*, **108**, 919–948.

Schätti, B. & Schmitz, A. (2006). Re-assessing *Platyceps ventromaculatus* (Gray, 1834) (Reptilia: Squamata: Colubrinae). *Revue Suisse de Zoologie*, **113**, 747–768.

Schätti, B. & Trape, J. F. (2008). *Bamanophis*, a new genus for the west African colubrid *Periops dorri* Lataste, 1888 (Reptilia: Squamata: Colubrinae). *Revue Suisse de Zoologie*, **115**, 595–615.

Schätti, B., Tillack, F. & Helfenberger, N. (2009). A contribution to *Spalerosophis microlepis* JAN, 1865, with a short review of the genus and a key to the species (Squamata: Serpentes: Colubridae). *Herpetozoa*, **22**, 115–135.

Sinaiko, G., Magory-Cohen, T., Meiri, S. & Dor, R. (2018). Taxonomic revision of Israeli snakes belonging to the *Platyceps rhodorachis* species complex (Reptilia: Squamata: Colubridae). *Zootaxa*, **4379**, 301–346.

Smith, M. A. (1928). The status of some recently described genera and species of snakes. *Annals and Magazine of Natural History*, **1** (series 10), 494–497.

Smith, M. A. (1943). *The Fauna of British India, Ceylon and Burma, Including the Whole of the Indo-Chinese Region*. *Vol*. *III*. *Serpentes*. London, Taylor and Francis.

Spawls, S., Howell, K., Hinkel, H. & Menegon, M. (2018). *Field Guide to East African Reptiles*. London, Bloomsbury.

Stamatakis, A. (2014). RAxML Version 8: A tool for phylogenetic analysis and post-analysis of large phylogenies. *Bioinformatics*, **30**, 1312–1313.

Szunyoghy, J. V. (1932). Beiträge zur vergleichenden Formenlehre des Colubridenschädels, nebst einer kraniologischen Synopsis der fossilen Schlangen Ungarns. Mit nomenclatorischen, systematischen und phyletischen Bemerkungen. *Acta Zoologica*, **13**, 1–56.

Szyndlar, Z. & Rage, J. C. (2002). Fossil records of the true vipers, pp. 419–444 *in*: Schuett, G. W., Höggren, M., Douglas, M. E. & Greene, H. W. (eds) *Biology of the Vipers*. Eagle Mountain, Eagle Mountain Publishing LC.

Thompson, J. D., Higgins, D. G. & Gibson, T. J. (1994). clustal W: improving the sensitivity of progressive multiple sequence alignment through weighting, position-specific gap penalties and weight matrix choice. *Nucleic Acids Research*, **22**, 4673–4680.

Underwood, G. (1967). *A contribution to the classification of snakes*. London, Trustees of the British Museum (Natural History).

Utiger, U., Schätti, B. & Helfenberger, N. (2005). The Oriental colubrine genus *Coelognathus* Fitzinger, 1843 and classification of old and new world racers and ratsnakes (Reptilia, Squamata, Colubridae, Colubrinae). *Russian Journal of Herpetology*, **12**, 39–60.

Wall, F. (1913). A popular treatise on the common Indian snakes. Part 22. *Journal of the Bombay Natural History Society*, **23**, 34–43.

Vaidya, G., Lohman, D. J. & Meier, R. (2011). sequencematrix: concatenation software for the fast assembly of multi-gene datasets with character set and codon information. *Cladistics*, **27**, 171–180.

Wade, E. (2001). Review of the False Smooth snake genus *Macroprotodon* (Serpentes, Colubridae) in Algeria with a description of a new species. *Bulletin of the Natural History Museum London* (*Zoology*), **67**, 85-107.

Wall, F. (1921). *Ophidia Taprobanica or the Snakes of Ceylon*. Colombo, H. R. Cottle.

Wall, F. (1924). A Hand-List of the Snakes of the Indian Empire. Part II. *Journal of the Bombay Natural History Society*, **29**, 598–632.

Wallach, V., Williams, K. L. & Boundy, J. (2014). *Snakes of the World*. *A Catalogue of Living and Extinct Species*. Boca Raton, CRC Press.

Werneburg, I. & Sanchez-Villagra, M. R. (2015). Skeletal heterochrony is associated with the anatomical specializations of snakes among squamate reptiles. *Evolution*, **69**, 254–263.

Werner, F. (1924). Neue oder wenig bekannte Schlangen aus dem Naturhistorischen Staatsmuseum in Wien. *Sitzungsberichte der Koeniglichen Akademie der Wissenschaften, Wien*, **133**, 29–56.

Whitaker, R. & Captain, A. (2004). *Snakes of India, the Field Guide*. Chengalpattu, Draco Books.

Wilson, L. D. (1967). Generic reallocation and review of *Coluber fasciolatus* Shaw (Serpentes: Colubridae). *Herpetologica*, **23**, 260–275.

ZooBank Registration

at www.zoobank.org

Present article: The LSID for this publication is as follows: urn:lsid:zoobank.org:pub:F3C885C4-8BB4-4259-B01D-9C0B-6D044DEC

Appendix 1

Osteological materials (including the voucher specimen for molecular taxonomy):

Argyrogena fasciolata: LSUMNS 9524 ('Pakistan'), LSUMNS 34120, NHMUK 1930.5.8.420 ('Bombay Presidency'), NHMUK 1930.5.8.421 ('Thana, India'), NHMUK 1930.5.8.423 ('Hosar, near Bangalore'), PUZ 322 (voucher specimen for molecular taxonomy; dry skull plus wet preserved specimen)

Eirenis decemlineatus: AMNH R-68159 ('Palestine')

Hemorrhois nummifer: UMMZ Herps-67200 (MorphoSource Media: M29188)

Hierophis gemonensis: NHMUK 1930.5.8.416

Hierophis viridiflavus: AMNH R-67986, NHM 1964.1196 ('France')

Lytorhynchus diadema: FMNH 164704 ('Egypt')

Lytorhynchus maynardi: FMNH 167666 ('Pakistan')

Orientocoluber spinalis: AMNH R-4974, NHMUK 1930.5.8.413

Platyceps collaris: UMMZ Herps-127487 ('Croatia') (MorphoSource Media: M29180)

Platyceps florulentus: AMNH R-21795 ('Egypt'), FMNH 153054 ('Egypt'), NHMUK uncatalogued ('Egypt')

Platyceps rhodorachis: AMNH R-85578 ('Karachi, Pakistan')

Platyceps variabilis: NHMUK 1930.3.7.5 ('Dthala, Aden Hinterland')

Platyceps ventromaculatus: NHMUK 1930.5.8.392-393 ('Chitral'), NHMUK 1930.5.8.394 ('Chitral')

Spalerosophis diadema cliffordii: AMNH R21793 ('Tunisia'), FMNH 22777, FMNH 153046 ('Egypt')

Appendix 2

Table 1. Used partitioning scheme.

Partition name	**Model**
12S ribosomal DNA	GTR + I + G
16S ribosomal DNA	GTR + I + G
COI 1st codon position	SYM + G
COI 2nd codon position	F81 + I
COI 3rd codon position	TVM + G